Prolinate-based heterogeneous catalyst for Knoevenagel condensation reaction: Insights into mechanism reaction using solid-state electrochemical studies

Josefa Ortiz-Bustos, Paula Cruz, Yolanda Pérez [*], Isabel del Hierro [*]

COMET-NANO Group. Departamento de Biología, Geología, Física y Química Inorgánica, ESCET, Universidad Rey Juan Carlos, Móstoles, Madrid 28933, Spain

A B S T R A C T

The carbon-carbon bond formation is essential to producing relevant organic compounds that exhibit pharmacological and biological properties. In this regard, Knoevenagel and multicondensation reactions have been employed to test the acid-base cooperativity of functionalized mesoporous silica nanoparticles with L-prolinate based groups (Prol-MSN) in comparison with choline hydroxide fragments (Chol-MSN). Thus, Prol-MSN material has shown to be a promising heterogeneous organocatalyst for condensation reactions. The use of electrochemical sensor techniques allowed through cyclic and differential pulse voltammetry studies a better understanding of the catalytic mechanism of Knoevenagel reaction for the Prol-MSN material, including the role of silanol surface groups and protic solvents.

1. Introduction

Synthetic chemists, whose major objective is the synthesis of new compounds or the implementation of new reactions to prepare well-known compounds more efficiently, have joined relatively late the practice of green chemistry principles in comparison to analytical or chemical-physical chemists whose discoveries of monitoring pollution devices or modelling mechanism of polluting systems date from far back in time. One of the milestones of the synthetic chemistry branch has been the development of a new concept to define the success of a chemical reaction, the atom economy has replaced the yield term to quantify, not just the fraction of reactant that ends up in the final product, but also implicitly the potential existence of by-products. Following green chemistry principles, a 100% atom economy process is most desirable [1]. In this context, multicomponent condensation reactions have focused huge attention from the research community, not just due to the demand for feedstock molecules for the synthesis of highly valuable compounds or drugs, but also because these reactions possess the appropriate characteristics to be performed in the presence of heterogeneous catalysts following most of the items imposed by the green chemistry principles [2–5]. It is sufficient to take a glance at the last decade's literature to find contributions about this topic in journals on different research fields such as catalysis, organic and inorganic materials (e.g., COFs and MOFs), organic synthesis, natural products, etc. [6–9] Two reviews recently published, by Van Schijndel and co-workers [10] and by Appaturi and co-workers [11], cover this field. In the first case, an interesting overview of Knoevenagel reaction through history is performed, catalysts diversity and its associated mechanisms open new research opportunities and update this reaction in the context of green chemistry. The second review focuses on heterogeneous catalysts used in Knoevenagel reaction (including zeolites, hybrid mesoporous silicas and metal oxides) and provides an interesting survey of chemical and engineering aspects.

We have previously published the synthesis of hybrid mesoporous silica nanoparticles based on the ligand choline hydroxide and its application as an efficient basic catalyst in several C-C bond formation reactions. In this work, we want to go a step further using this material as a starting point and through an easy-to-work acid-base reaction we have prepared L-proline functionalized mesoporous silica nanoparticles. The amino acid L-proline is a well-known organocatalyst due to its properties as Brønsted acid or/and Brønsted base and its ability to generate iminium or enamine intermediates that are typical of covalent organocatalysis [12]. L-Proline and L-proline derivatives have been extensively used as catalysts of multicomponent reactions performed in aqueous media to produce synthetically and biologically relevant heterocycles, an important type of organic compounds that form part of
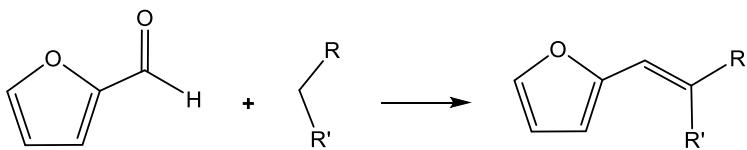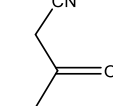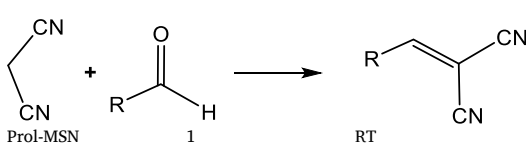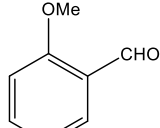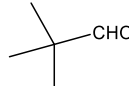
Table 1
Knoevenagel condensation reactions[a].

Entry	Catalyst[a]	Time (h)	Temperature (°C)	Reactant	Conversion (%)[b]	Selectivity (%)[c]
1	Prol-MSN	0.5	RT	malononitrile (CN, CN)	99	100
2	Chol-MSN				99	100
3	Prol-MSN	4	40	ethyl cyanoacetate (CN, EtO C=O)	97	100
4	Chol-MSN				99	100
5	Prol-MSN	4	40	ethyl acetoacetate / acetylacetone (EtO C=O, Me)	70	Isomers E/Z 42/28
6	Chol-MSN				68	37/31
7	Prol-MSN	1	RT	o-anisaldehyde (OMe, CHO)	99	100
8	Prol-MSN	4	RT	pivalaldehyde (CHO)	99	100

[a] 0.25 mol% catalyst and 10 mmol reactants, ethanol as solvent.
[b] Conversion determined by GC [c] Products isolated and characterized by ^{1}H NMR.

more than 60% of agrochemicals and drugs [13]. Also, choline hydroxide and related ionic liquids have been widely applied in the field of green, sustainable chemistry, and many chemical processes [14]. In particular, the ionic liquid [Choline] [Pro] (2-hydroxyethyl)-trimethyl-ammonium (S)−2-pyrrolidinecarboxylic acid salt) has demonstrated to be a highly active catalyst that exhibits a low selectivity for direct aldol reactions between paranitrobenzaldehyde and acetone in aqueous solution, yielding a mixture of compounds from the first and second aldol reaction [15]. An ionic liquid-supported L-proline derivative has also been tested as a catalyst in the same reaction, but it requires 30 mol% of catalyst, higher time, and temperature to render comparable results [16]. More recently, in the graphene oxide (GO)/Fe$_3$O$_4$/L-proline nanohybrid system, the L-proline is introduced through the non-covalent immobilization via hydrogen bonding interaction between the L-proline and the GO/Fe$_3$O$_4$ nanocomposite, achieving a useful and highly recyclable catalyst for the preparation of bis-pyrazole derivatives [17]. The ionic liquid 1-ethyl-3-methylimidazolium-(S)−2-pyrrolidine carboxylic acid salt or [EMIm] [Pro], which possesses (S)-proline as an anion, facilitates the asymmetric Michael addition reaction via the enamine mechanism [18]. Guan et al. have demonstrated by preparing 2-(3-(triethoxysilyl)propylcarbamoyl)pyrrolidine-functionalized SBA-15 and Al-SBA-15, amongst other amine functionalities, the synergic effect between the acid and the base in bifunctional materials showing that weak acid matching weak base is beneficial to the Knoevenagel and nitroaldol condensation reactions [19]. Recently, the synthesis of organic-inorganic hybrid materials based on silyl-derivatives with basic functionalities such as amino, diamino and pyrrolidine

molecules or pyrazolium and imidazolium hydroxides, has been achieved through post-synthetic grafting procedures on the surface of silica M41S-type and successfully tested as catalysts in Knoevenagel reaction [20].

In this work, the application as heterogeneous organocatalysts of hybrid mesoporous silica nanoparticles materials, functionalized with choline hydroxide (Chol-MSN) and with L-proline units (Prol-MSN), has been developed in a set of condensation reactions to compare both functionalities and understand the influence of their basic strength. Additionally, a cooperative mechanism reaction for the Knoevenagel condensation has been proposed based on solid-state cyclic and differential pulse voltammetry studies and inspired by the experimental approach used when preparing electrochemical sensors.

2. Experimental section

2.1. Materials

Tetraethylortosilicate (TEOS) 98%, (3-glycidyloxypropyl)trimethoxysilane), trimethylamine solution 4.2 M in ethanol, hexamethyldisilazane, malononitrile, ethyl cyanoacetate, 5,5-dimethylcyclohexane-1,3-dione, ammonium acetate, acetylacetone, ethyl acetoacetate, pivalaldehyde, o-anisaldehyde and benzaldehyde, were purchased from Sigma Aldrich and used as received. Hexadecyltrimethylammonium bromide (CTBA) was purchased from Acros and used as received. Toluene, dichloromethane, and furfural were purchased from SDS and Aldrich, respectively, distilled and dried from appropriate drying agents

Table 2
Different multicondensation reactions.

Entry	Catalyst[a]	Time (h)	Temperature (°C)	Yield (%)[b]
1	Chol-MSN	2	RT	97
2	Prol-MSN	2	RT	91

Entry	Catalyst[c]	Time (h)	Temperature (°C)	Yield (%)[d]
3	Chol-MSN	2	60	82
4	Prol-MSN	2	60	85

[a] 0.25 mol% catalyst, 5 mmol reactants, and ethanol as solvent.
[b] Product isolated and characterized by ^{1}H NMR.
[c] 1.25 mol% catalyst, 2 mmol dimedone, 1 mmol benzaldehyde and 1.2 mmol ammonium acetate, ethanol as solvent.
[d] Compound isolated and characterized by ^{1}H NMR.

before being used. Ethanol (synthesis quality) was purchased from SDS and used as received. Milli-Q water was used in the experiments. The mesoporous silica nanoparticles (MSN) and glycidoxypropyl functionalized mesoporous silica nanoparticles Gly-MSN were synthesized as previously published [21].

2.2. Preparation of catalysts

2.2.1. Preparation of MSN functionalized with choline hydroxide functionality (Chol-MSN)

2.0 g of the previously prepared Gly-MSN was suspended in water and treated with a solution of trimethylamine 4.2 M in ethanol (4 mmol, 0.95 mL). The suspension was heated at 50 °C and stirred for 48 h. The resulting white solid, labelled as Chol-MSN, was obtained by filtration, and washed with ethanol (2 × 30 mL). The solid was dried under vacuum and stored in air.

2.2.2. Preparation of MSN functionalized with proline functionality (Prol-MSN)

1.0 g of the previously prepared Chol-MSN was suspended in water and treated with a Proline aqueous solution (2 mmol, 0.23 g). The suspension was stirred for 16 h. The resulting white solid, labelled as Prol-MSN, was obtained by filtration, and washed with ethanol (2 × 30 mL). The solid was dried under vacuum and stored in air.

2.3. Characterization

X-ray diffraction (XRD) patterns of the silicas were obtained on a Phillips Diffractometer model PW3040/00 X'Pert MPD/MRD at 45 KV and 40 mA, using Cu-Kα radiation (λ = 1.5418 Å). N_2 gas adsorption-desorption isotherms were obtained using a Micromeritics TriStar 3000 analyser, and pore size distributions were calculated using the Barret-Joyner-Halenda (BJH) model on the adsorption branch. Infrared

spectra were recorded on a Nicolet-550 FT-IR spectrophotometer (in the region 4000 to 400 cm-1) as KBr disks. ^{1}H NMR spectra were recorded on a Varian Mercury FT-400 spectrometer. Cross Polarization ^{13}C CP/MAS NMR spectra were recorded on a Varian-Infinity Plus 400 MHz Spectrometer operating at 100.52 MHz proton frequency (4 μs 90° pulse, 4000 transients, spinning speed of 6 MHz, contact time 3 ms, pulse delay 1.5 s). Elemental analyses were carried out by the Microanalytical Service of the Universidad Complutense de Madrid. The C, H, and N analyses were accomplished by combustion analysis with elemental microanalyzers LECO CHNS-932. Scanning electron micrographs and morphological analysis were carried out on an XL30 ESEM Philips. The electrochemical studies were performed with a potentiostat/galvanostat Autolab PGSTAT302 Metrohm.

2.4. Condensation reactions

For Knoevenagel reaction, 10 mmol of aldehyde compound (furfural, o-anisaldehyde or pivalaldehyde) 10 mmol of methylene activated compound (malononitrile, ethyl cyanoacetate or ethyl acetoacetate), and 50 mg of organocatalyst in ethanol (5 mL total final volume) or solventless were mixed in a 50 mL tube and then, the mixture was stirred at different temperatures (see Tables 1 and 3). After reaction completion, 5 mL of dichloromethane was added to dilute the organic compounds. The solid catalyst was precipitated by centrifugation and separated from the liquid phase. To analyse the sample by gas chromatography, 1 mL of sample was withdrawn and diluted in ethanol to 5 mL, and a fixed amount of dodecane, as internal standard. The sample was analysed by GC-FID (Agilent 6890 N, DB-Wax capillary column 30 m, 0.53 mm). In addition, the corresponding compounds obtained after C-C condensation reactions were recrystallized from ethyl acetate and checked by ^{1}H NMR (See supplementary material). A similar procedure was followed for multicomponent reactions but using benzaldehyde, dimedone and malononitrile or ammonium acetate (see Table 2).
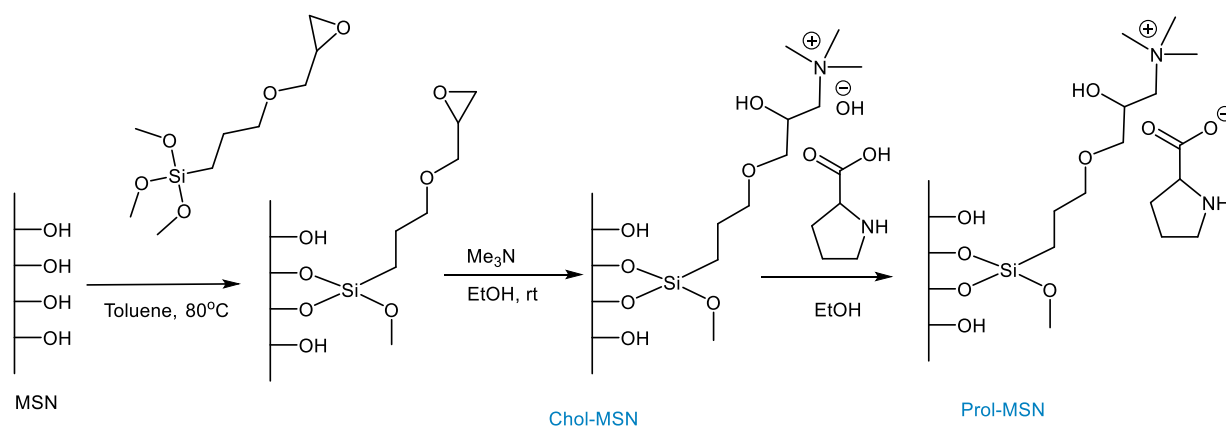
Scheme 1. Immobilization of choline hydroxide and L-proline functionalities onto mesoporous silica nanoparticles.
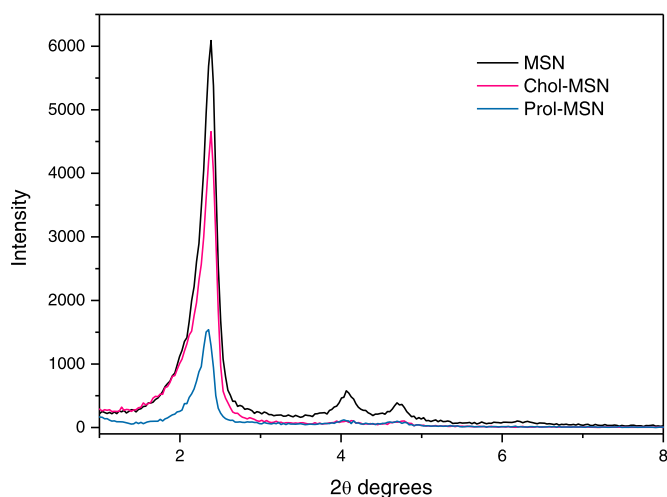
Fig. 1. Small-angle XRD patterns of Chol-MSN, Prol-MSN catalysts, and pristine MSN.

3. Results and discussion

The industrial production of choline hydroxide includes reacting at a temperature above 30 °C ethylene oxide and trimethylamine in an aqueous medium. Similarly, here we have prepared a silane ligand containing the choline hydroxide functionality from 3-glycidyloxy-propyl)trimethoxysilane and trimethylamine to get the epoxide opening and the subsequent quaternization of the amine. Our research group has published previously the synthesis of hybrid mesoporous nanoparticles by co-condensation methodology following the sol-gel process principles by using TEOS and this silane ligand as silicon sources [22]. In this work, we have followed an alternative way, the epoxide functionality has been immobilized onto mesoporous silica nanoparticles followed by the reaction with trimethylamine to synthesize the material labelled as Chol-MSN from now on. In a second step, by a straightforward acid-base reaction in aqueous media, the choline hydroxide has been neutralized with an equimolar amount of L-proline (See Scheme 1) to prepare hybrid mesoporous nanoparticles with this functionality on the silica surface (labelled as Prol-MSN). As an alternative route to prepare these materials, the synthesis of the ligands following homogeneous workup procedures and their subsequent immobilization can be performed as confirmed by ^{1}H NMR studies (See Fig. S1).

3.1. Catalysts characterization

The mesostructure of both materials was confirmed by small-angle

XRD, N$_2$ adsorption-desorption isotherms and SEM analysis. Unmodified MSN shows a well-resolved pattern at low 2θ values with one strong (100) diffraction peak at 2.37 and two additional high order peaks (110) and (200) with lower intensities at 4.08 and 4.72; corresponding to a highly ordered hexagonal mesoporous silica. The MSN materials containing the ionic liquid functionality showed the same pattern, indicating that the ordered mesoporous structure of MSN was well retained after the post-synthesis functionalization process. The plane (100) in the pristine MSN shows higher intensity compared with the hybrid materials Chol-MSN and Prol-MSN, which can be attributed to the low local order, due to variations in the wall thickness of the framework and the reduction of scattering contrast between the channel wall and the ligands present on the inner surface of silica materials (see Fig. 1). SEM micrographs show that the spherical framework of MSN is well preserved after functionalization, as can be seen in Fig. 2. (A). Besides, pristine MSN and Prol-MSN mesoporous silica spheres are uniform in shape and size diameter.

The physical parameters such as the surface area (S$_{BET}$), total pore volume, and BJH average pore diameter have been measured by nitrogen adsorption experiments. The characteristic type IV BET isotherms for the prepared materials show the presence of mesoscale pores. The sharp N$_2$ condensation step at P/P$_o$ = 0.2–0.4 for MSN-type materials indicates that the supports have a highly ordered hexagonal pore system. The parent MSN material possesses S$_{BET}$ (1041 m^2 g^{-1}), a pore volume of 0.84 cm^3 g^{-1} and a BJH pore diameter of 32 Å. The material Chol-MSN presents an important decrease in the S$_{BET}$, (825 m^2 g^{-1}) pore volume (0.50 cm^3 g^{-1}) and average BJH pore diameter (24 Å) in comparison with the parent support due to the presence of choline hydroxide functionality anchored to the channels which partially block the adsorption of nitrogen molecules. An additional capillary condensation step above P/P$_0$ > 0.9 is observed, suggesting the formation of interparticle porosity and the increase of aggregation. Similar type IV N$_2$ adsorption-desorption isotherm, characteristic of mesoporous materials, is obtained for the material Prol-MSN (see Fig. 3). In this case, the further decrease observed for S$_{BET}$, pore-volume, and pore diameter agrees with the higher size requirements imposed by the L-proline unit in comparison to hydroxide. Based on the nitrogen content obtained by elemental analysis, the number of molecules attached to the mesoporous MSN was calculated to be 0.51 and 0.49 mmol g^{-1} for Chol-MSN and Prol-MSN, respectively (L$_o$ =%N/nitrogen molecular weight). This data indicates the quantitative reaction of the choline hydroxide unit with the amino acid and its total consumption, which means that the only functionality available on the silica surface of Prol-MSN is the L-proline unit itself. Considering L$_o$ and S$_{BET}$ of the mesoporous silica nanoparticles, the average surface density, d, of attached molecules and the average intermolecular distance are calculated to be as 0.29 and 1.85 molecules/nm^2 for Chol-MSN and 0.28 and 1.87 molecules/nm^2 for Prol-MSN, respectively.
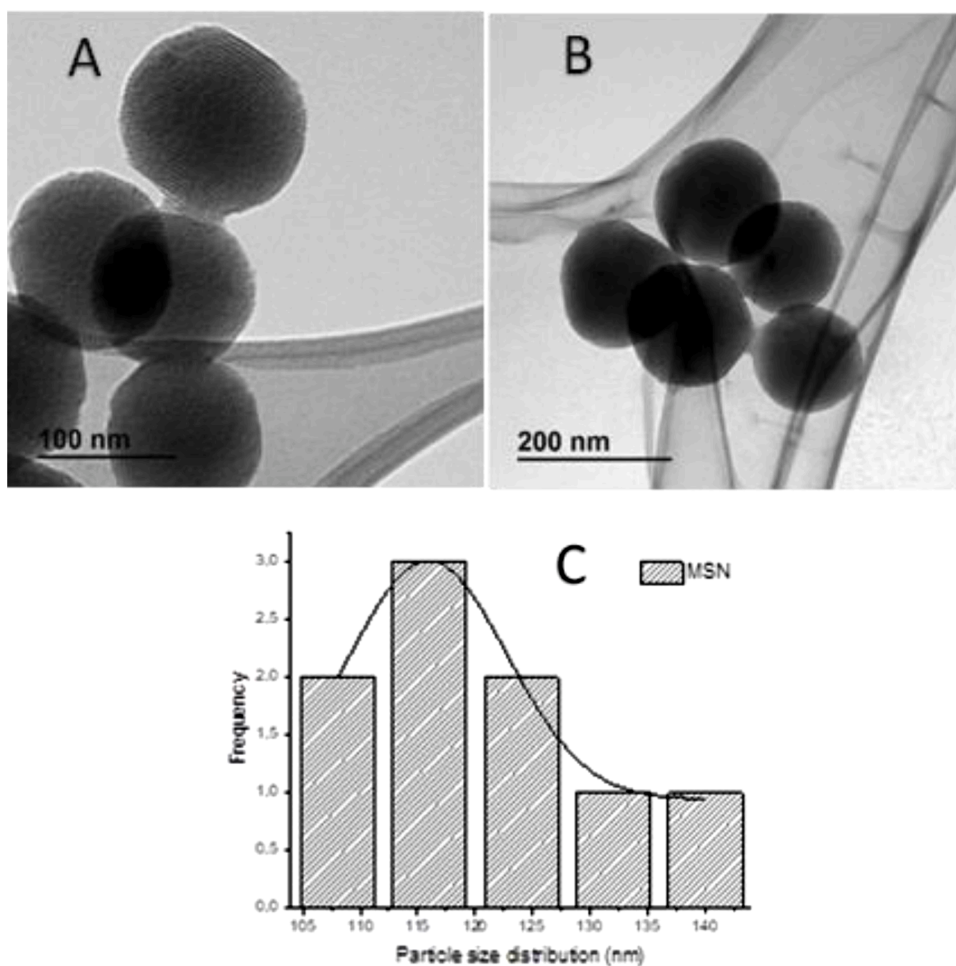
Fig. 2. (A) TEM micrograph of Prol-MSN (B) TEM micrograph of pristine MSN and (C) size distribution histogram of pristine MSN.
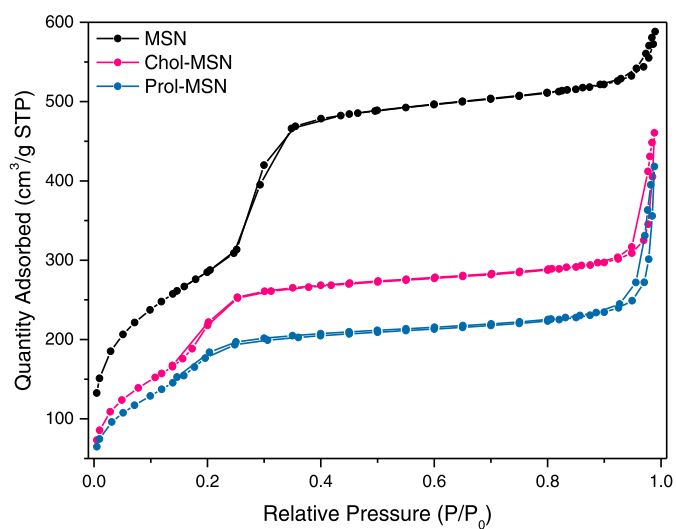

Fig. 3. Nitrogen adsorption/desorption isotherms of MSN, Chol-MSN, and Prol-MSN materials. Type IV isotherms typical of mesoporous silica are exhibited.

Fig. 4. ^{13}C CP MAS NMR of Prol-MSN and Chol-MSN catalysts.

The ^{13}C MAS NMR spectrum of Chol-MSN gives proof of the presence of the organic functionality linked to the silica surface (Fig. 4). After L-proline incorporation, some changes are observed. The ^{13}CP MAS NMR spectrum of Prol-MSN exhibits signals at 6, 22, and 71 ppm associated with the carbon atoms of the propyl chain -Si-CH_2-, -CH_2-CH_2-CH_2- and -CH_2-CH_2-CH_2-O, respectively. The signal attributed to the methylene group O-CH_2-CHOH- appears at 71 ppm (overlapped) and the signals due to carbon atoms of the opened epoxide function appear at 66 and 72 ppm, for methine CH-OH and methylene N–CH_2– groups, respectively.
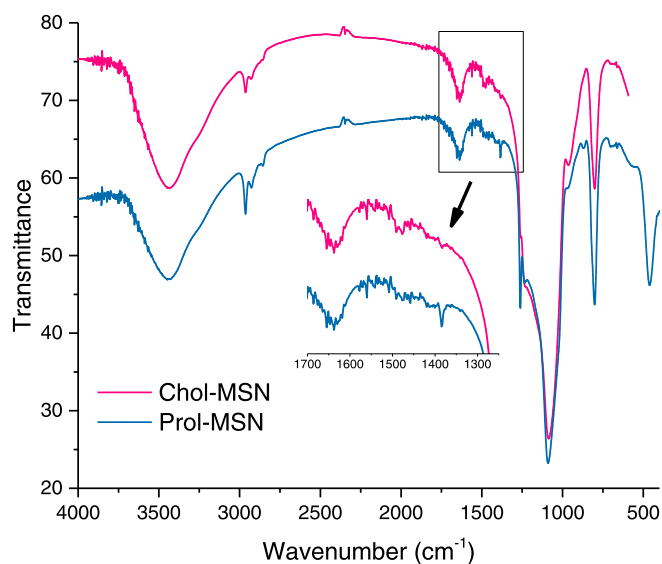
Fig. 5. FTIR spectra of Chol-MSN and Prol-MSN catalysts.

to the L-prolinate anion (see Fig. S2).

3.2. Catalytic tests

The potential applicability of the as-synthesized materials as organocatalysts for different C–C bond-forming reactions, such as Knoevenagel reaction and multicondesation reactions to prepare relevant products [23], is noticeable due to their basic properties. Hybrid organosilica materials are fully understood as heterogeneous catalysts due to the synergic properties offered by the Si-O-Si-OH framework and the organic functionality attached to the silica surface. In this sense, the basic functionalities typology on the silica surface is broad, in this work two basic functionalities Choline hydroxide and L-proline have been implemented by heterogenization onto MSN and tested to establish the difference, if any, between them. Choline hydroxide in the homogenous phase is defined as a transfer catalyst used to carry the hydroxide ion into organic systems and it is considered a strong base. L-proline is a well-known homogeneous organocatalyst due to its characteristics as Brønsted acid or/and Brønsted base and its ability to generate iminium or enamine covalent intermediates.

3.2.1. Knoevenagel reactions

The Knoevenagel condensation using furfural and several activated methylene compounds as reactants was carried out in a 50 mL reactor with 50 mg of catalyst, equivalent to 0.026 and 0.025 mmol of hydroxide choline and L-prolinate units for Chol-MSN and Prol-MSN, respectively, and with an equimolar amount of reactants (10 mmol). These reactions were performed on a gram scale by using approximately 0.25 mol% of catalyst to demonstrate the large-scale use. The results for Knoevenagel condensation reaction using furfural as reactant, summarized in Table 1, should allow assessing the basic strength of the tested catalysts. It is well known that the abstraction of a proton from methylene compound with a high value pK_a required the presence of a catalyst possessing strong basic properties. As can be seen, both catalytic systems work excellently in the condensation reaction using malononitrile ($pK_a = 11.4$) (Entries 1 and 2). The expected product is obtained quantitatively in a short time at room temperature using ethanol as solvent. The time conversion plot for the reaction is quite similar for both catalysts, although the activity is slightly enhanced for the Prol-MSN system (See Fig. S3). In the case of less activated ethyl cyanoacetate ($pK_a = 13.1$), the material Chol-MSN reaches a total conversion of the reactants at 40 °C increasing the reaction time to 4 h (Entry 4), meanwhile, Prol-MSN also exhibits an excellent conversion value (97%) under similar conditions (Entry 3). Using ethyl acetoacetate ($pK_a = 14.2$) conversions of 70% and 68% are achieved for Prol-MSN and Chol-MSN catalysts, respectively (Entries 5 y 6). Although the conversion obtained is similar for both materials, the selectivity towards the E isomer is more significant using the Prol-MSN system, obtaining a ratio

Two additional peaks at 15 and 59 ppm are assigned to the ethoxide unreacted group of the organic ligand CH_3CH_2-O-. The resonance peak at ca. 54 ppm indicates the presence of methyl groups attached to the nitrogen atom. Finally, additional small peaks at 28, 45, and 172 ppm are assigned to the C atoms of the C_4H_8N ring, and the -COO$^-$ group of the L-prolinate anion.

The FT-IR spectrum of mesoporous MSN after functionalization is shown in Fig. 5. The FTIR spectrum of MSN shows characteristic bands at 3441 cm^{-1} assigned to O-H stretching vibrations and the remaining physiosorbed water molecules, at 1629 cm^{-1} due to deformation vibrations of the adsorbed water molecules and at 1082, 959, and 806 cm^{-1} attributed to the Si-O stretching vibrations. Chol-MSN material displays additional bands at 2929 and 2878 cm^{-1} due to the ν(C–H) stretching vibrations and at 1489, 1471 cm^{-1} assigned to the bending vibrations of δ(C–H) of the alkyl chain. The FT-IR spectrum of pristine L-proline shows typical carboxylate (COO$^-$) asymmetric and symmetric stretching bands at 1622 and 1380 cm^{-1}. In comparison, the FTIR spectrum recorded for Prol-MSN shows similar bands, the first band corresponding to the L-proline fragment overlaps with the physiosorbed water band, but the second one is seen at 1383 cm^{-1} supporting the presence of the prolinate anion. The DRUV-Vis spectra of both materials show slight changes in the absorption band of the Chol-MSN material after reaction with L-proline. The weak absorption band due to the hydroxide choline functionality is observed at 263 cm^{-1}, after modification this band disappears, and a new one at 249 cm^{-1} appears assigned

Table 3
Furfural and acetylacetone condensation reaction.

Entry	Catalyst	Time (h)	Temperature (°C)	Conversion (%)[c]	Selectivity (%)[c]
1	Chol-MSN[a]	4	100	31	100
2	Prol-MSN[a]	4	100	43	100
3	Prol-MSN[b]	4	60	95	100

[a] 1.5 mol% catalyst and 3 mmol reactants in solventless conditions.
[b] 1.5 mol% catalyst and 3 mmol reactants in ethanol.
[c] Conversion and selectivity determined by ^{1}H NMR.
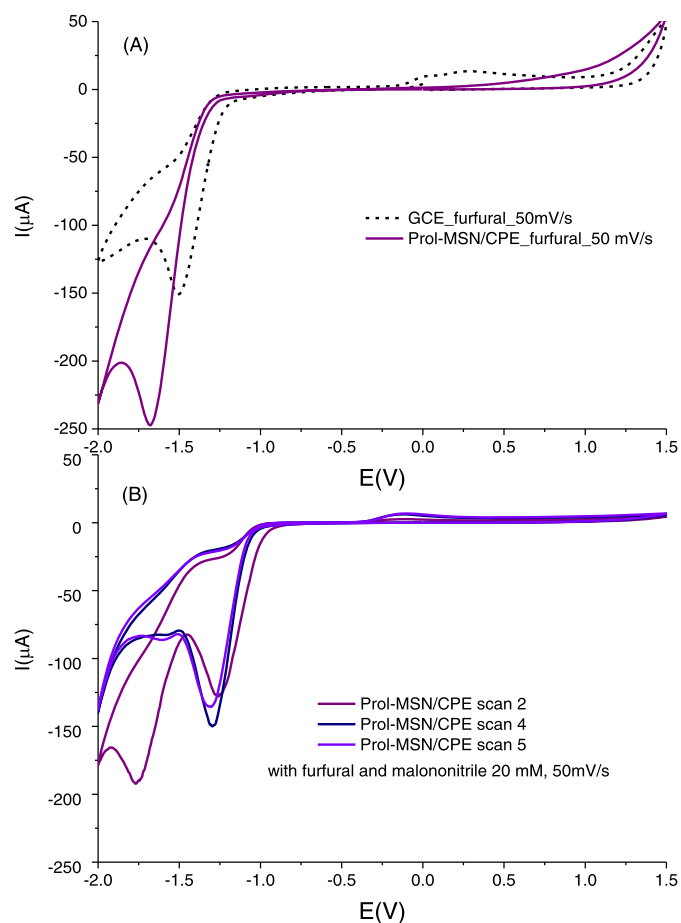
Fig. 6. Cyclic voltammogram of furfural (a) measured by using as working electrode a bare glassy carbon GCE and a modified carbon paste electrode with Prol-MSN material, Prol-MSN/CPE and (b) in the presence of malononitrile by using as working electrode a modified carbon paste electrode with Prol-MSN material (three consecutive scans). In 0.1 M Na$_2$HPO$_4$–NaH$_2$PO$_4$ solution (pH 7.4) as electrolyte vs Ag/AgCl/KCl (3 M) as reference electrode.

of 1.5:1 in comparison to the ratio 1.2:1 rendered by Chol-MSN material. To get a deeper knowledge about the catalytic properties of Prol-MSN material, additional reactants were employed to condensate with malononitrile and form other α,β-unsaturated products. For instance, when aromatic benzaldehyde or less activated o-anisaldehyde were used the reaction was quantitative in a short period at room temperature (Entry 7). If aliphatic aldehydes are used the results are different. The reaction is quantitative in the presence of the sterically hindered pivalaldehyde (Entry 8) but does not proceed in the presence of phenyl propionaldehyde.

Both organocatalysts were also successfully tested in the synthesis of 2-amino-4H-chromene and acridinedione derivatives (Table 2). The formation of 2-amino-4H-chromene derivate was efficiently achieved by both materials, reaching an excellent yield (Entries 1 and 2) in comparison to other systems. For instance, Keshavarz and co-workers reported a lower catalytic activity using a high ratio of catalyst /substrate (10 mol%) under reflux conditions [24] with the catalytic system consisting of L-Proline, immobilized by ionic interaction between the carboxylate group of L-prolinate, and the quaternary ammonium group of the cationic resin amberlite IRA900OH. In the formation of acridinedione derivative, the yield obtained by Prol-MSN catalyst is slightly superior to that obtained with Chol-MSN catalyst (Entries 3 and 4).

Furthermore, to extent of the utility of these systems, we tested both materials in the reaction of furfural and acetylacetone (pK$_a$ = 13.3) under solventless conditions, forming 3-(2-furylmethylene)−2,4-

pentanedione which is employed as a jet fuel precursor. As can be seen in Table 3, the reaction takes place selectively with better conversion for the catalyst Prol-MSN (Entries 1 and 2). In ethanol, it achieves a 95% yield with Prol-MSN as catalyst (Entry 3). This reaction has been also performed by other authors using MCM-41-alanine as a catalyst under solventless conditions rendering 88% conversion after 6 h [25] and with pyridine immobilized on magnetic silica to give 94% conversion, although with a notably higher catalyst/substrate ratio (0.2 g catalyst and 2 mmol substrates) [26].

### 3.3. Mechanistic studies by solid-state electrochemistry

It is well known that secondary amines are stronger bases than primary amines. The pyrrolidine functionality is considered a strong base in organic catalysis and explained why the chiral L-proline amino acid (pK$_{a2}$ = 10.6) and its derivatives have been extensively used in organocatalysis. L-proline can promote a very broad diversity of transformations due to the multiple catalytic roles granted by its structural features. In this work, the synthetic procedure allows the immobilization of the L-prolinate anion through the ionic pair interactions with the quaternary ammonium cation available in the choline moiety, so L-prolinate with a secondary amine functionality may behave as a nucleophile towards carbonyl groups, generating iminium cation intermediates that are characteristic of covalent organocatalysis. [27]

In the case of the Chol-MSN system where hydroxide choline functionality acts as a strong base, we have previously established an ion pair mechanism for Knoevenagel reaction [22]. In a similar ion-pair mechanism to that proposed for Chol-MSN, the material Prol-MSN acting as a strong base may abstract the proton from the methylene carbon with the subsequent formation of a carbanion, which would attack the carbonyl group forming an enol intermediate. The reaction would finish with the formation of a double C=C and water release (See Fig. S4). Depending on the nature of the substituent groups in the methylene compound (electronic properties) proton abstraction is more or less favoured and, therefore, requires a catalyst with higher or lower basicity, so, it is possible to correlate the basicity of the catalyst with the pK$_a$ of the methylene reactant. In this work, the condensation of furfural takes place quantitatively with activated compounds, and the conversion decreases as the pK$_a$ of the reactants increases, as expected. However, the conversion of the reaction with acetylacetone renders a lower conversion than expected based only on its pK$_a$ value (13.3). An alternative mechanism (See Fig. S5) would also explain the good performance of this catalyst in the Knoevenagel condensation reaction of relatively weak bases with limited proton abstraction ability, especially when high pK$_a$ demanding methylene compounds are considered. In this mechanism basic L-prolinate anion with a secondary amine function may force the formation of a hemiaminal intermediate by the addition of the amine group to the carbonyl group of the aldehyde, in this case, the efficiency of the catalysts does not correlate with the pK$_a$ of their amine group [28].

To gain insights into the reaction mechanism, solid-state voltammetry studies were performed and, considering the efficiency shown for the materials tested in this work, Prol-MSN was chosen as a representative system. Thus, cyclic voltammetry (CV) and Differential Pulse Voltammetry (DPV) measurements were performed to study the electrochemical response of redox L-prolinate ligand tethered to the walls of mesoporous silica nanoparticles. The experiments were carried out at room temperature, using a three-electrode-single compartment electrochemical cell comprising of a modified carbon paste as working electrode, an Ag/AgCl/KCl 3 M reference electrode, and a platinum rod counter electrode. Firstly, the material Prol-MSN was characterized by cyclic voltammetry being the working electrode a carbon paste modified electrode CPE which was prepared by mixing the appropriate amount of graphite, hybrid silica-based material and nujol as an agglutinant agent and by packing the so prepared carbon paste into the end of Teflon cylindrical tube, equipped with a screwing stainless-steel piston to
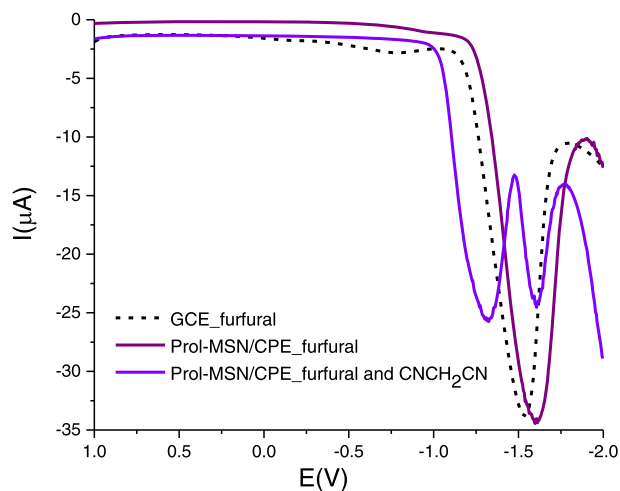
Fig. 7. Differential Pulse voltammogram (25 mV modulation amplitude) of furfural measured by using as working electrode (a) GCE (b) Prol-MSN/CPE and (c) in the presence of malononitrile by using Prol-MSN/CPE as working electrode. In 0.1 M Na_2HPO_4–NaH_2PO_4 solution (pH 7.4) as electrolyte vs Ag/AgCl/KCl (3 M) as reference electrode.
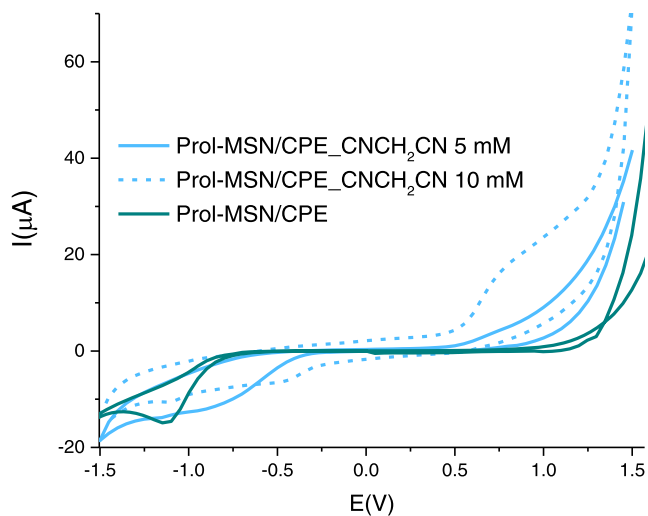
Fig. 8. Cyclic voltammogram of malononitrile 5 mM and 10 mM concentration measured by using Prol-MSN/CPE as working electrode in 0.1 M Na_2H-PO_4–NaH_2PO_4 solution (pH 7.4) as electrolyte vs Ag/AgCl/KCl (3 M) as reference electrode.

provide inner electrical contact. Prol-MSN/CPE material shows an irreversible reduction peak around −1.14 V with a low peak current and without the presence of an anodic wave associated (Fig. S6). To corroborate that this peak is correctly attributed to the L-prolinate anion, a similar measurement was performed at lower pH where the pyrrolidine unit is protonated. As expected, the voltammogram shows an irreversible reduction peak shifted towards higher potentials (less negative) since at this pH value the protonated L-prolinate ligand requires a less energetic potential for the reduction as compared to the more electron-rich pyrrolidine unit (Fig. S6). Then, the behaviour of the Prol-MSN material with the reactants used in the Knoevenagel reaction was studied by using the Prol-MSN/CPE to perform cyclic voltammetry measurements in the presence of 20 mM furfural (Fig. 6A) or in the presence of both reactants, furfural and malononitrile, simultaneously (Fig. 6B).

Fig. 6A displays the CV curves of a solution containing 20 mM furfural in a 0.1 M Na_2HPO_4–NaH_2PO_4 solution (pH 7.4) recorded at the

Table 4
Solvent effect for Knoevenagel condensation of furfural with malononitrile[a].

Solvent	Catalyst Prol-MSN Conversion (%)	Selectivity (%)		Prol-HMDS-MSN Conversion (%)	Selectivity (%)	
Ethanol	99	100	–	80	100	–
Water	81	100	–	79	100	–
Solventless	76	100	–	43	100	–
Toluene	66	98	2	23	58	42
Dichloromethane	35	66	34	12	57	43

[a] 0.25 mol% catalyst and 10 mmol reactants at room temperature for 30 min. [b] Products quantified by ^{1}H NMR (See Fig S9).
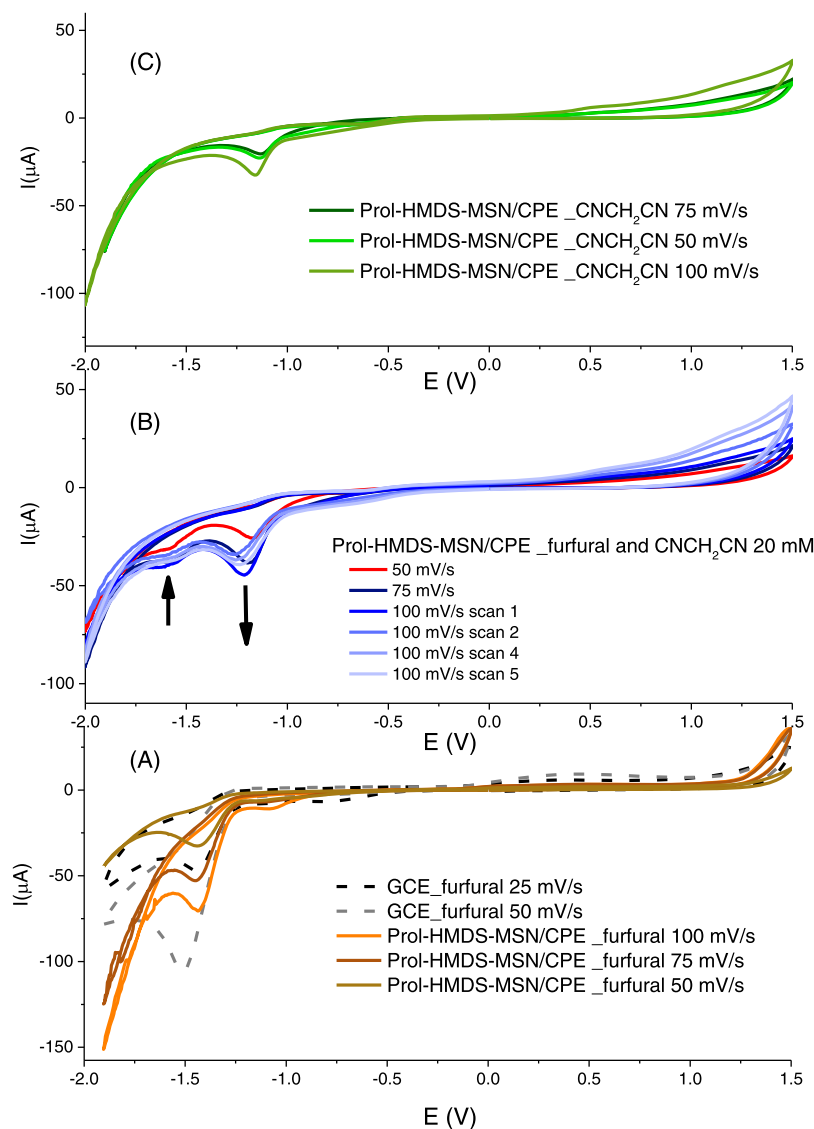
**Fig. 9.** Cyclic voltammogram of (A) furfural and (C) malononitrile measured by using as working electrode GCE and Prol-HMDS-MSN/CPE (B) furfural and malononitrile simultaneously measured by using as working electrode Prol-HMDS-MSN/CPE. In 0.1 M Na$_2$HPO$_4$–NaH$_2$PO$_4$ solution (pH 7.4) as electrolyte vs Ag/AgCl/KCl (3 M) as reference electrode.

bare GCE and Prol-MSN/CPE. Furfural can be electrochemically reduced into furfuryl alcohol [29], the cathodic scan shows an irreversible peak without any peak associated in the reversal scan. By using the Prol-MSN/CPE electrode, the peak is located at −1.68 mV which is 18 mV more negative than that obtained with the bare GCE and the cathodic peak current is also larger. Similar electrocatalytic activity for furfural was also found in the DPV results (Fig. 7), which occurs with an increased peak current and a higher overpotential at the Prol-MSN/CPE compared with that at the bare GCE, indicating the improved sensing ability of Prol-MSN/CPE as electrochemical sensor. The shift of the reduction peak associated with furfural to more negative potential suggests an increase of electron density on the carbonyl group of the aldehyde, which can be interpreted as the existence of an interaction between the basic pyrrolidine unit present in the catalyst and furfural, and points to the addition of the amine group to the carbonyl group of the furfural as the initial step of the Knoevenagel reaction mechanism. The electroreduction of furfural in the presence of malononitrile (20 mM) renders a new peak associated with the formation of the condensation compound accompanied by a dramatic decrease of the peak associated with furfural as shown in Fig. 6B. This fact has been corroborated by the performance of a cyclic voltammogram of pure

2-(furan-2-ylmethylene)malononitrile, this compound shows an irreversible cathodic peak around −1.25 V when its CV is measured by using both working electrodes, bare GCE and Prol-MSN/CPE (see Fig. S7), which suggests the existence of any interaction between this compound and the L-prolinate unit in the catalyst. Similar electrocatalytic activity for furfural in the presence of malononitrile was also found in the DPV results, which occurs with the appearance of a new peak associated with the condensation compound, meanwhile, the peak current due to furfural decreases immediately after applying the electrical current (See Fig. 7).

To investigate a plausible activation of malononitrile by the Prol-MSN catalyst a similar study was conducted. In this case, the CV of pure malononitrile measured by GCE is silent in the cathodic scan and it shows a broad peak in the oxidation scan overlapped with the limit imposed by the solvent oxidation (See Fig. S8). This behaviour allows understanding the performance of Prol-MSN material in the presence of these reactants in the cathodic region from 0 to −1.5 V. As depicted previously, a reduction peak attributed to the L-prolinate unit is detected at −1.14 V in Prol-MSN/CPE, in the presence of malononitrile this peak shifts to more positive potentials and simultaneously an important decrease in the peak current takes place, being the decrease in the
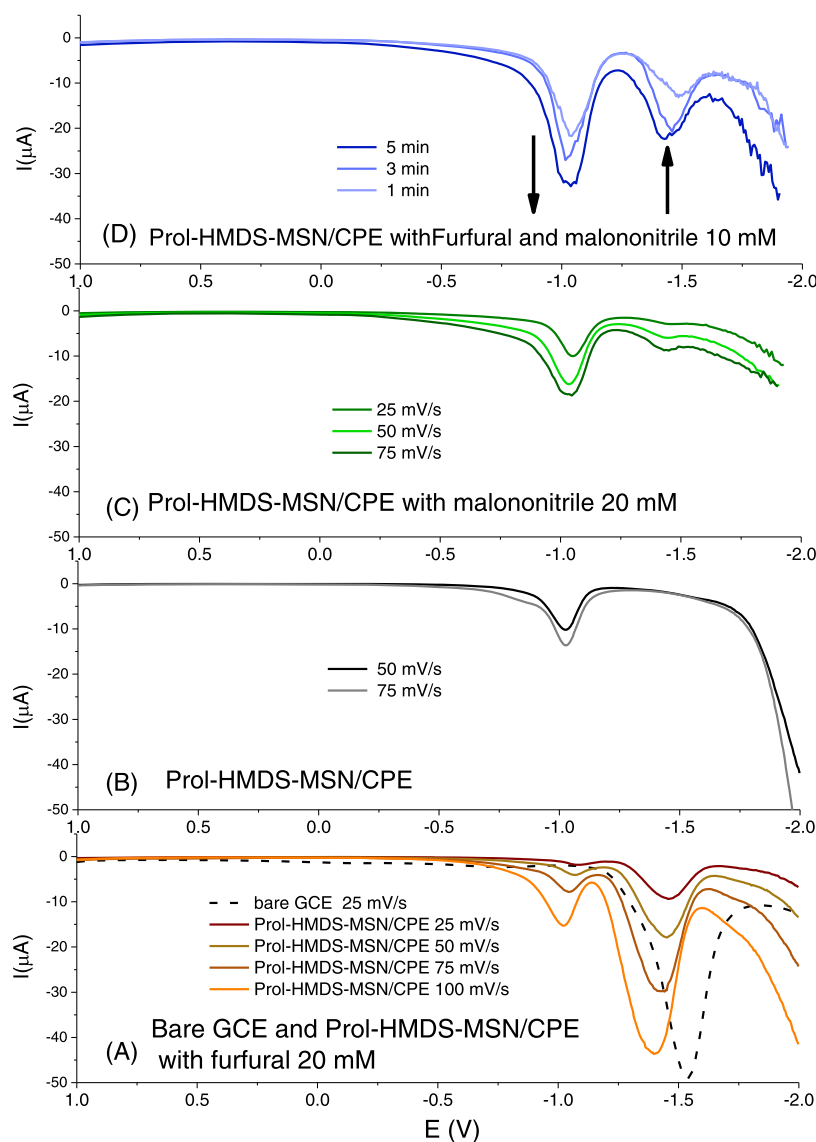
Fig. 10. Differential Pulse voltammogram of (A) furfural measure by using as working electrode a bare GCE and Prol-MSN/CPE (B) Prol-HMDS-MSN/CPE at different values of modulation amplitude (C) Prol-HMDS-MSN/CPE in the presence of malononitrile and (D) Prol-HMDS-MSN/CPE in the presence of furfural and malononitrile at different times. In 0.1 M Na$_2$HPO$_4$–NaH$_2$PO$_4$ solution (pH 7.4) as electrolyte vs Ag/AgCl/KCl (3 M) as reference electrode.

current height more pronounced at higher concentration of malononitrile (See Fig. 8). This data supports the active role of the catalyst in the deprotonation of the methylene compound and the influence of the basic strength of the catalyst since an acid−base equilibrium is established related to the pK$_a$ of malononitrile and L-prolinate.

To go further inside the plausible mechanism established with Prol-MSN material as a catalyst the effect of the solvent was also studied in the Knoevenagel condensation reaction of furfural and malononitrile. As can be seen in Table 4, there is an important influence of the solvent on the reaction. Protic solvents such as water and ethanol render the highest yields. It is also significant the result obtained under solventless conditions. On the contrary, using a non-polar solvent such as toluene or an organic polar solvent such as dichloromethane led the reaction through a completely different path since the yield of the reaction decreases significantly and 2-furoic acid is obtained as a side product because of the oxidation of furfural. These results support the formation of a carbanion and/or an iminium intermediate which reach a major stabilization in polar solvents like ethanol. Additionally, to understand if this material acts as a bifunctional catalyst due to the presence of acidic silanol groups onto the silica surface (isoelectric point of silica goes

from 1.5 to 3.5) a similar catalyst, name hereafter as Prol-HMDS-MSN, was prepared end-capping the surface silanol groups with trimethylsilyl groups by reaction with hexamethyldisilazane and tested under similar experimental conditions. The results obtained show an analogous influence of the solvent in the catalytic reaction, but the conversion of furfural to 2-(furan-2-ylmethylene)malononitrile or to 2-furoic acid is lower than that obtained with Prol-MSN in all sets of experiments proven that silylated catalysts result in an important loss of activity. In addition, to establish the effect of the catalyst, a set of blank experiments were performed by mixing furfural and acetylacetone under different experimental conditions. The Knoevenagel condensation reaction renders a very low conversion in ethanol (6% conversion) and the same conversion value was observed in presence of MSN and ethanol under reflux. When the reaction was performed without solvent and the temperature was increased until 100 °C the conversion achieved 24% without MSN and 13% in the presence of MSN, being this last result lower than expected due to diffusional problems. Although these values are not negligible are far away from that obtained in the presence of the catalyst under identical experimental conditions.

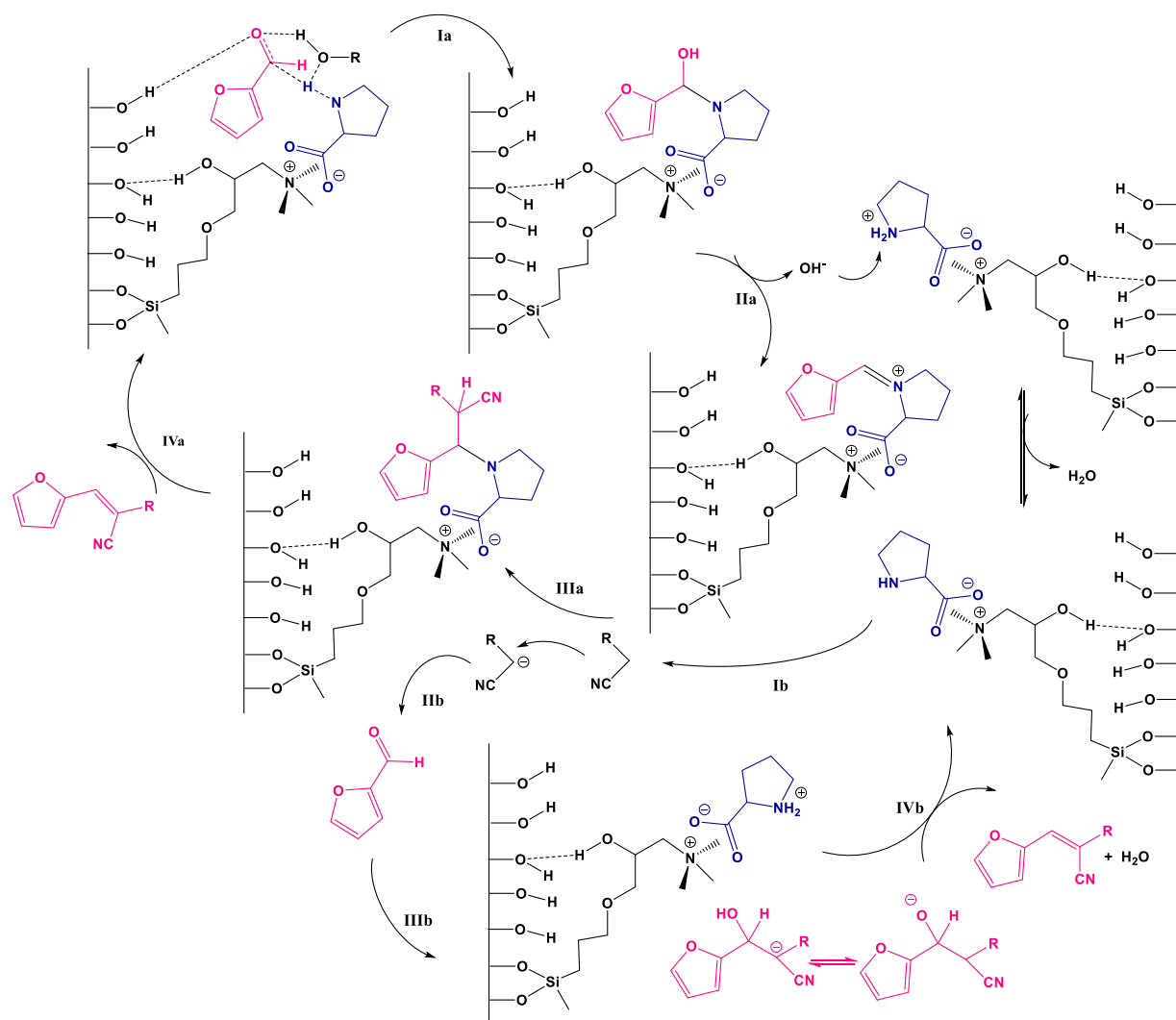Additional electrochemical solid-state experiments were performed

Fig. 11. Cooperative Mechanism Proposal for Knoevenagel Condensation of furfural and methylene compounds with Prol-MSN catalyst.

by using Prol-HMDS-MSN to prepare carbon paste working electrodes to study the electrochemical condensation of furfural and malononitrile (See Figs. 9 and 10). The CV performed for the modified carbon paste electrode prepared with this material Prol-HMDS-MSN/CPE shows, as expected, an irreversible cathodic peak around −1.14 V with a low current peak attributed to the reduction of the L-prolinate unit (See Figs. S10 and 10C). In addition, Fig. 9A shows the CV measured with this electrode in the presence of furfural (20 mM) and for comparison purposes, the CV measured with bare GCE. As can be seen, at comparable scan speed values, the peak current of the reduction peak at −1.43 V, attributed to furfural, decreases significantly when measured with Prol-HMDS-MSN/CPE in comparison with the peak at −1.51 V measured with bare GCE, which indicates a lower sensitivity of the former electrode and lower adsorption ability of furfural, probably due to the hydrophobic character of the silica surface in comparison to Prol-MSN/CPE. The shift of the reduction peak of furfural towards more positive potential values (from −1.51 to −1.43 V) suggests a decrease in the electron density of the carbon atom in the carbonyl group of furfural. Based on these data, it can be inferred that the lack of interaction between furfural and the silanol groups on the silica surface influences the electron density on furfural. The presence of protic solvent still makes possible the formation of an intermediate furfural-solvent which would facilitate the attack of the basic L-prolinate anion, however, the electron density donation from the base to the carbonyl group would not be as efficient as with Prol-MSN. Finally, Fig. 9B shows the electroreduction of

furfural in the presence of malononitrile (both 10 mM), in this CV the peak attributed to furfural at −1.43 V has decreased significantly and a new peak at −1.20 V (overlapped with that attributed to prolinate unit) appears due to the formation of the condensation compound.

This hypothesis can be supported by the DPV voltammetry studies. Fig. 10B shows the DPV measured with Prol-HMDS-MSN/CPE where the cathodic peak attributed to the L-prolinate appears at −1.14 V. As can be observed in Fig. 10A and 10C this peak remains unaltered in the presence of furfural or malononitrile. Finally, the electroreduction of furfural in the presence of malononitrile (both 10 mM) was studied (Fig. 10D), the reaction causes a new peak at −1.12 V associated with the formation of the condensation compound accompanied by a dramatic decrease of the peaks at −1.43 V associated with furfural (Fig. 10A). The disappearance of this wave is an acceptable clue for relatively complete consumption of furfural.

The results indicate that the surface silanol groups, and in less extension the hydroxyl group available in the alkyl chain ligand used to tether the L-prolinate unit to the silica surface, intervene in the reaction mechanism, making Prol-MSN material an acid−base bifunctional catalyst which promotes a cooperative catalytical mechanism. Considering the results obtained in this work and theoretical studies previously published [30], we hypothesize the establishment of hydrogen-bridge interactions of silica surface silanol groups with the carbonyl group of the reactants making them more susceptible to nucleophilic reactions [31,32]. This interaction, together with the protic solvent participation,
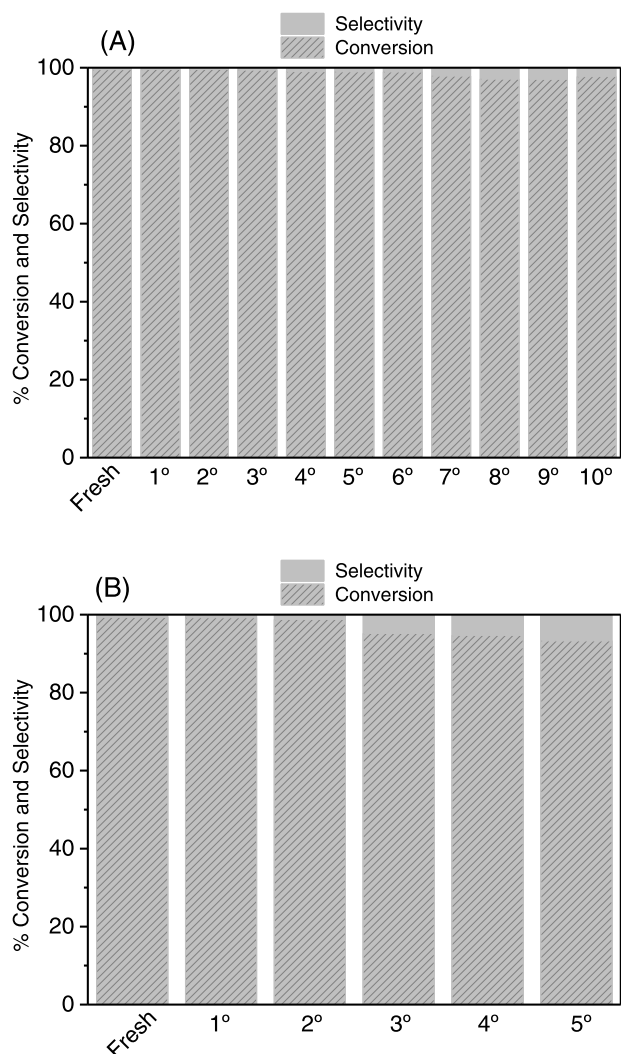
Fig. 12. The catalytic activity of Prol-MSN for Knoevenagel condensation of furfural (a) with malononitrile in 10 consecutive runs and (b) with ethyl cyanoacetate in 5 consecutive runs.

initiates the mechanism reaction by the formation of carbinolamine intermediate which loses a hydroxide ion and forms a cationic iminium intermediate. Simultaneously, the catalyst acting as a strong base abstracts the proton from the methylene carbon with the subsequent formation of a carbanion, which would attack the carbonyl group forming an enolate intermediate. In this mechanism path, the hydroxide ion regenerates the catalyst by water release. This route is an acid−base equilibrium and hence will be dependant on the pK_a of reactant and catalyst. Once the enolate and iminium ions are formed, the next step is the nucleophilic attack of enolate to iminium. The last step of the mechanism is the regeneration of the catalyst (See Fig. 11).

3.4. Recycling tests

Since one of the highest benefits of heterogeneous catalysts is its recoverability and reused, we tested the properties of the efficient Prol-MSN catalyst to verify its stability and the absence of L-prolinate loss during the catalytic process. The experimental essays show that the Prol-MSN catalyst was easily recovered by centrifugation and reuse without any additional treatment. As depicted in Fig. 12 the conversion and selectivity values are retained for Knoevenagel condensation of furfural and malononitrile during 10 consecutive runs. In the case of condensation of furfural with ethyl cyanoacetate, a slight decrease in

conversion is observed after five consecutive runs, which can be explained by the loss of catalyst by additional work-up since in this case the product must be dissolved for its isolation and then, the catalyst separated by filtration.

4. Conclusions

Hybrid mesoporous silica nanoparticles synthesized using post grafting procedures and containing ionic (choline and Proline) basic sites, have been successfully synthesized and evaluated as catalysts in different condensation reactions. The catalytic activity of both functionalities is comparable, but the mechanism of action seems to be different. A cooperative mechanism for Prol-MSN catalyst has been proposed employing solid-state electrochemical techniques. The presence of silanol groups in the framework of the support promotes a cooperative electrophilic activation of furfural and makes possible the formation of iminium intermediates stable in polar solvents. Simultaneously the catalyst Prol-MSN intervenes in a classical ion-pair path, due to its basic strength the catalyst abstracts a proton from the activated methylene compound and forms an enolate. The achieved results show that the synthetic strategy allows generating active hybrid materials that combine basic sites with other acid structural functions to generate multisite catalysts for carrying out one-pot multistep catalytic processes.

CRediT authorship contribution statement

Josefa Ortiz-Bustos: Investigation, Data curation, Formal analysis, Software. **Paula Cruz:** Data curation, Investigation. **Yolanda Pérez:** Conceptualization, Supervision, Writing – review & editing. **Isabel del Hierro:** Conceptualization, Supervision, Investigation, Data curation, Formal analysis, Writing – original draft, Writing – review & editing.

Declaration of Competing Interest

The authors declare that they have no known competing financial interests or personal relationships that could have appeared to influence the work reported in this paper.

Acknowledgements

Supplementary materials

Supplementary material associated with this article can be found, in the online version, at doi:10.1016/j.mcat.2022.112328.

References

[1] S.E. Manahan, Green Chemistry and the Ten Commandments of Sustainability, 2nd ed., ChemChar Research, Inc Publishers, Columbia, Missouri U.S.A., 2006.

[2] R. Takakura, K. Koyama, M. Kuwata, T. Yamada, H. Sajiki, Y. Sawama, Hydroquinone and benzoquinone-catalyzed aqueous Knoevenagel condensation, Org. Biomol. Chem. 18 (2020) 6594–6597, https://doi.org/10.1039/D0OB01397H.

[3] S. Preeti, K. Nand, Metal-free multicomponent reactions: a benign access to monocyclic six-membered N-heterocycles, Org. Biomol. Chem. 19 (2021) 2622–2657, https://doi.org/10.1039/D1OB00145K.

[4] M.M. Heravi, F. Janati, V. Zadsirjan, Applications of Knoevenagel condensation reaction in the total synthesis of natural products, Monatshefte Chem. 151 (2020) 439–482, https://doi.org/10.1007/s00706-020-02586-6.

[5] R.W. Armstrong, A.P. Combs, P.A. Tempest, S.D. Brown, T.A. Keating, Multiple-component condensation strategies for combinatorial library synthesis, Acc. Chem. Res. 29 (1996) 123–131, https://doi.org/10.1021/ar9502083.

[6] B.M. Al-Shehri, M.R. Shabaan, M. Shkir, A. Kaushik, M.S. Hamdy, Single-step fabrication of Na-TUD-1 novel heterogeneous base nano-catalyst for Knoevenagel condensation reaction, J. Nanostruct. Chem. 11 (2020) 259–269, https://doi.org/10.1007/s40097-020-00364-8.

[7] A.H. Chughtai, N. Ahmad, H.A. Younus, A. Laypkov, F. Verpoort, Metal–organic frameworks: versatile heterogeneous catalysts for efficient catalytic organic

transformations, Chem. Soc. Rev. 44 (2015) 6804–6849, https://doi.org/10.1039/C4CS00395K.

[8] A. Dhakshinamoorthy, N. Heidenreich, D. Lenzen, N. Stock, Knoevenagel condensation reaction catalysed by Al-MOFs with CAU-1 and CAU-10-type structures, CrystEngComm 19 (2017) 4187–4193, https://doi.org/10.1039/C6CE02664H.

[9] N. Anbu, R. Maheswari, V. Elamathi, P. Varalakshmi, A. Dhakshinamoorthy, Chitosan as a biodegradable heterogeneous catalyst for Knoevenagel condensation between benzaldehydes and cyanoacetamide, Catal. Commun. 138 (2020), 105954.

[10] K. van Beurden, S. de Koning, D. Molendijk, J. van Schijndel, The Knoevenagel reaction: a review of the unfinished treasure map to forming carbon–carbon bonds, Green Chem. Lett. Rev. 13 (2020) 349–364, https://doi.org/10.1080/17518253.2020.1851398.

[11] J.N. Appaturi, R. Ratti, B.L. Phoon, S.M. Batagarawa, I.U. Din, M. Selvaraj, R. J. Ramalingam, A review of the recent progress on heterogeneous catalysts for Knoevenagel condensation, Dalton Trans. (2021) 11–21, https://doi.org/10.1039/D1DT00456E.

[12] B.S. Vachan, M. Karuppasamy, P. Vinoth, S. Vivek Kumar, S. Perumal, V. Sridharan, J.C. Menéndez, Proline and its derivatives as organocatalysts for multi- component reactions in aqueous media: synergic pathways to the green synthesis of heterocycles, Adv. Synth. Catal. 362 (2020) 87–110, https://doi.org/10.1002/adsc.201900558.

[13] H. Tan, H. Liu, X. Chen, H. Chen, S. Qiu, Racemic total synthesis of dactyloidin and demethyldactyloidin through the dl-proline-catalyzed Knoevenagel condensation/[4 + 2] cycloaddition cascade, Org. Biomol. Chem. 13 (2015) 9977–9983, https://doi.org/10.1039/C5OB01636C.

[14] B.L. Gadilohar, G.S. Shankarling, Choline based ionic liquids and their applications in organic transformation, J. Mol. Liq. 227 (2017) 234–261, https://doi.org/10.1016/j.molliq.2016.11.136.

[15] S. Hu, T. Jiang, Z. Zhang, A. Zhu, B. Han, J. Song, Y. Xie, W. Li, Functional ionic liquid from biorenewable materials: synthesis and application as a catalyst in direct aldol reactions, Tetrahedron Lett. 48 (2007) 5613–5617, https://doi.org/10.1016/j.tetlet.2007.06.051.

[16] C. Zhuo, D. Xian, W. Jian-Wei, X. Hui, An efficient and recyclable ionic liquid-supported proline catalyzed Knoevenagel condensation, ISRN Org. Chem. 2011 (2011), https://doi.org/10.5402/2011/676789 pp 676789-5.

[17] M. Keshavarz, A. Zarei Ahmady, L. Vaccaro, M. Kardani, Non-covalent supported of l-proline on graphene Oxide/Fe₃O₄ nanocomposite: a novel, highly efficient and superparamagnetically separable catalyst for the synthesis of bis-pyrazole derivatives, Molecules 23 (2018) 330, 10.3390/molecules23020330.

[18] X. Zheng, Y. Qian, Y. Wang, Direct asymmetric aza Diels–Alder reaction catalyzed by chiral 2-pyrrolidinecarboxylic acid ionic liquid, Catal. Commun. 11 (2010) 567–570, https://doi.org/10.1016/j.catcom.2009.12.021.

[19] J. Guan, B. Liu, X. Yang, J. Hu, C. Wang, Q. Kan, Immobilization of proline onto Al-SBA-15 for C–C bond-forming reactions, ACS Sustain. Chem. Eng. 2 (2014) 925–933, https://doi.org/10.1021/sc4005247.

[20] A. Erigoni, M.C. Hernández-Soto, F. Rey, C. Segarra, U. Díaz, Highly active hybrid mesoporous silica-supported base organocatalysts for CC bond formation, Catal. Today 345 (2020) 227–236, https://doi.org/10.1016/j.cattod.2019.09.041.

[21] J. Ortiz-Bustos, Y. Pérez, I. Hierro, Structure, stability, electrochemical and catalytic properties of polyoxometalates immobilized on choline-based hybrid mesoporous silica, Microporous Mesoporous Mater. 321 (2021), 111128, https://doi.org/10.1016/j.micromeso.2021.111128.

[22] I. Hierro, Y. Pérez, M. Fajardo, Supported choline hydroxide (ionic liquid) on mesoporous silica as heterogeneous catalyst for Knoevenagel condensation reactions, Microporous Mesoporous Mater. 263 (2018) 173–180, https://doi.org/10.1016/j.micromeso.2017.12.024.

[23] A. Dömling, W. Wang, K. Wang, Chemistry and biology of multicomponent reactions, Chem. Rev. 112 (2012) 3083–3135, https://doi.org/10.1021/cr100233r.

[24] M. Keshavarz, N. Iravani, M.H. Ahmadi Azqhandi, S. Nazari, Ion-pair immobilization of L-prolinate anion onto cationic polymer support and a study of its catalytic activity as an efficient heterogeneous catalyst for the synthesis of 2-amino-4H-chromene derivatives, Res. Chem. Intermed. 42 (2016) 4591–4604, https://doi.org/10.1007/s11164-015-2302-0.

[25] J.N. Appaturi, M. Selvaraj, S.B. Abdul Hamid, Synthesis of 3-(2-furylmethylene)-2,4-pentanedione using DL-Alanine functionalized MCM-41 catalyst via Knoevenagel condensation reaction, Microporous Mesoporous Mater. 260 (2018) 260–269, https://doi.org/10.1016/j.micromeso.2017.03.031.

[26] K. Tarade, S. Shinde, S. Sakate, C. Rode, Pyridine immobilised on magnetic silica as an efficient solid base catalyst for Knoevenagel condensation of furfural with acetyl acetone, Catal. Commun. 124 (2019) 81–85, https://doi.org/10.1016/j.catcom.2019.03.005.

[27] A. Khalafi-Nezhad, E.S. Shahidzadeh, S. Sarikhani, F. Panahi, A new silica-supported organocatalyst based on L-proline: an efficient heterogeneous catalyst for one-pot synthesis of spiroindolones in water, J. Mol. Catal. A Chem. 379 (2013) 1–8, https://doi.org/10.1016/j.molcata.2013.07.009.

[28] P. Moriel, E.J. García-Suárez, M. Martínez, A.B. García, M.A. Montes-Morán, V. Calvino-Casilda, M.A. Bañares, Synthesis, characterization, and catalytic activity of ionic liquids based on biosources, Tetrahedron Lett. 51 (2010) 4877–4881, https://doi.org/10.1016/j.tetlet.2010.07.060.

[29] Q. Wang, J. Zhang, Y. Xu, Y. Wang, L. Wu, X. Weng, C. You, J. Feng, A one-step electrochemically reduced graphene oxide based sensor for sensitive voltammetric determination of furfural in milk products, Anal. Methods 13 (2021) 56–63, https://doi.org/10.1039/D0AY01789B.

[30] E.V. Dalessandro, H.P. Collin, L.G.L. Guimarães, M.S. Valle, J.R. Pliego, Mechanism of the piperidine-catalyzed Knoevenagel condensation reaction in methanol: the role of iminium and enolate ions, J. Phys. Chem. B 121 (2017) 5300–5307, https://doi.org/10.1021/acs.jpcb.7b03191.

[31] J. Lauwaert, E. De Canck, D. Esquivel, P. Van Der Voort, J.W. Thybaut, G.B. Marin, Effects of amine structure and base strength on acid–base cooperative aldol condensation, Catal. Today 246 (2015) 35–45, https://doi.org/10.1016/j.cattod.2014.08.007.

[32] S.L. Hruby, B.H. Shanks, Acid–base cooperativity in condensation reactions with functionalized mesoporous silica catalysts, J. Catal. 263 (2009) 181–188, https://doi.org/10.1016/j.jcat.2009.02.011.